Energy 251 (2022) 123978

Contents lists available at ScienceDirect

Energy

journal homepage: www.elsevier.com/locate/energy

A reliability-aware chance-constrained battery sizing method for island microgrid

Da Huo [a], Marcos Santos [b], Ilias Sarantakos [b], Markus Resch [c], Neal Wade [b], David Greenwood [b, *]

[a] School of Water, Energy and Environment, Cranfield University, Cranfield, MK43 0AL, UK
[b] School of Engineering, Newcastle University, Newcastle, NE1 7RU, UK
[c] Wirtschaftsagentur Burgenland Forschungs- und Innovations GmbH, Europastraße 1, A-7540, Güssing, Austria

ARTICLE INFO

Article history:
Received 3 August 2021
Received in revised form
3 March 2022
Accepted 9 April 2022
Available online 14 April 2022

Keywords:
Battery sizing
BESS
Chance-constrained programming
Distribution system
Island microgrid
Reliability
Second-order cone programming

ABSTRACT

Island Microgrids can coordinate local energy resources, provide post-fault reliability improvements for local customers, and aggregate local power and energy resources to offer services to the wider system. A crucial component of an Island Microgrid is the battery energy storage system, which can manage local imbalances, alleviate constraints, and improve reliability by enabling post-fault islanding. A planning and sizing method is required to quantify and maximize the benefits of battery energy storage while avoiding over-investment and under-utilization. This paper combines comprehensive reliability assessment with chance-constrained convex optimization, via second-order cone programming, to optimally size energy storage within an Island Microgrid. Chance constraints are applied to the battery state-of-charge to avoid sizing the energy storage to accommodate extreme cases of uncertainty, avoiding uneconomic investment. The probability of reaching a state-of-charge constraint also indicates the likelihood that the battery energy storage system will be unable to facilitate island operation in the event of an outage, which affects the Island Microgrid reliability. The method is demonstrated on a real Austrian distribution network as part of the MERLON project. Results illustrate that an optimal trade-off can be identified between system reliability and operating cost when the probability of violating the chance constraints is 4.8%.

1. Introduction

Traditional distribution networks are transitioning to active distribution systems with distributed energy resources (DERs) and intelligent energy management schemes [1]. This transition brings technical, social, and economic challenges driven by the uncertainties that renewable generators and low carbon technologies bring to supply and demand. Island microgrids (IM), which can maximize the use of renewable energy [2], improve supply reliability to customers [3], and coordinate local resources for participation in wider network and system ancillary services, are a potential solution to these challenges. However, these IM require appropriate planning methods to quantify the benefits they can deliver and ensure they are designed and operated in a cost-effective manner. This paper provides a novel planning and sizing method for IM which optimizes the capacity and operational strategy of a battery energy storage system (BESS), while minimizing the total cost of the system, and accounting for the system reliability at the same time.

1.1. Island microgrid

The IM, also referred as the Integrated Local Energy System [4], is a subset of the distribution network which can act as a virtual power plant when connected to the wider system and continue to operate in island mode when disconnected either intentionally for economic benefits, or due to a fault. The IM can optimally integrate the flexible resources and interconnections within local energy networks and ensure their operational and economic optimization [5]. A key component of IM is the Battery Energy Storage System (BESS) [6]; BESS enable IM to operate as energy islands after a fault on the wider distribution network which would otherwise result in customer disconnections [7]. BESS's fast ramp rates enable them to

* Corresponding author.
E-mail address: david.greenwood@newcastle.ac.uk (D. Greenwood).

https://doi.org/10.1016/j.energy.2022.123978

Nomenclature

A. Indices and sets

$t, \hat{t} \in T$	Time step
$i, k \in N$	Bus index

B. Parameters

D_T	Analyzed time period in days
$BESS_{CC,max}$	Maximum available budget for investing BESS
$BESS_{LT}$	BESS lifetime
d	Discount rate
C_{BESS}^{en}	BESS capacity unit cost (€/kWh)
C_{BESS}^{pwr}	BESS power rating unit cost (€/kW)
VOLL	Value of Lost Load (€/MWh)
Π_G	System electricity price (€/MWh)
Π_{re}	Renewable generator electricity price (€/MWh)
RG	Number of renewable generators
E_b^{stb}	BESS standby loss
A_{FR}	Available payment for providing frequency response (€/MW/h)
Δt	Length of a time step (hour)

C. Uncertainty variables

$\xi_{e,i}$	Load forecast error of bus i

D. Deterministic decision variables

u_i, R_{ik}, I_{ik}	Ancillary variables
P_G	Grid electricity import (MW)
$P_{re,i}$	Electricity import from renewable generator or grid of bus i (MW)
$P_{ch,de}$	Charging power (MW)
$P_{dis,de}$	Discharging power (MW)
$E_{b,de}$	Battery state of energy (MWh)
E_{BESS}	Battery capacity (MWh)
P_{BESS}	Battery power rating (MW)

E. Stochastic decision variables

$\tilde{P}_{ch}$	Charging power
$\tilde{P}_{dis}$	Discharging power

F. Reliability assessment parameters

$BESS_A$	Battery's annual unavailability
$BESS_{DS}$	Battery's discharge state
CAIDI	Customer Average Interruption Duration Index (hours)
SAIDI	System Average Interruption Duration Index (hours/customer/year)
Up_{time}	Simulated period at UP state
$DOWN_{time}$	Simulated period at DOWN state
λ_i	Failure rate of element k (failures/year)
r_i	Repair time of element k (hours/failure)
W	Weighting factor of linear decision rule
G_{ik}	Real part of element Y_{ik} in the admittance matrix
B_{ik}	Imaginary part of element Y_{ik} in the admittance matrix
$P_{LF,i}$	Forecasted active power load of bus i (MW)
$Q_{L,i}$	Reactive power load of bus i (Mvar)
$P_{re,i}$	Renewable generator active power output of bus i (MW)
$Q_{re,i}$	Renewable generator reactive power output of bus i (Mvar)
η_{ch}	Charging efficiency
η_{dis}	Discharging efficiency
K_w	Global wear coefficient
α, β	Probability of chance constraints violation
q	Quantile
T_{FR}	Hours committed to provide frequency response
$\xi_{e,s}$	Sum of all load forecast error
$P_{net,i}$	Net active power injection of bus i (MW)
$Q_{net,i}$	Net reactive power injection of bus i (Mvar)
C_{El}	Cost of importing electricity (€)
R_{FR}	Revenue of providing frequency response (€)
C_{RC}	Reliability cost (€)
V	Bus voltage (V)
θ	Bus phase angle (°)
$BESS_{CC}$	BESS capital cost (€)
$\tilde{E}_b$	Battery state of energy
EENS	Expected Energy Not Served (MWh/year)
MTTF	Mean Time to Failure (hours)
MTTR	Mean Time to Repair (hours)
U_1, U_2	Uniformly distributed random numbers between 0 and 1
U_k	Annual unavailability of element k (hours/year)
U_{BESS}	Annual unavailability of battery (hours/year)
L_k	Active power demand at load point k (MW)

execute rapid charging and discharging, which allows them to provide ancillary services such as primary frequency control [8], participate in the capacity market and dynamic firm frequency response services [9].

1.2. Optimal sizing for island microgrid – literature review

Quantifying the impact of the BESS capital and operational costs on benefits from ancillary services, energy trading, and network reliability improvement is a complex, multi-objective problem. In most methods within the existing literature, the optimal size of BESS is determined via revenue-based objectives with reliability as either an incidental bonus or a constraint using indices such as Loss of Load Expectation (LOLE) or Expected Energy Not Supplied (EENS). Examples include optimally sizing the BESS to minimize capital and operational costs while guaranteeing a level of reliability by meeting a specified LOLE criterion [10]; optimizing the capacity of a BESS for an IM to guarantee its reliability [11–13] size the BESS for off-grid systems which are respectively supported by wind and solar generation, the reliability indicator in the sizing studies must exceed a given threshold; and [14] uses a sequential Monte Carlo simulation (SMCS) based searching method for sizing the BESS to minimize cost and meet reliability requirements.

In some cases, the reliability benefit is included in the objective function, but these papers either use heuristic optimization methods or simplify the problem: the authors of [15] use a Genetic Algorithm, which is computationally intensive and does not guarantee a globally optimal solution, to optimize the size and location of BESS within a network. A separate process is required to calculate the optimal dispatch of BESS. Neither stage employs optimal power flow techniques. In Ref. [16], a robust optimal schedule is calculated for a BESS in an IM with the objective of minimizing the cost of operation (including the cost of load shedding during island operation); however, it deals only with operation, and sizing is excluded from the problem.

System reliability will often be in direct conflict with

maximizing revenue from energy trading and ancillary services, which necessitates a trade-off between the two objectives. This is because enhancing the availability of the BESS to improve reliability – either by designing it to have additional energy capacity or operating it far from its SoC limits – reduces the availability of power and energy resources to gain revenue via energy and ancillary service markets. This compromise between (capital and operational) costs and reliability enhancement has not been explicitly investigated in the existing literature, nor do any published methods identify an optimal trade-off.

The reliability evaluation methods in existing BESS planning and sizing studies often yield an over-optimistic estimate for the system reliability because, for example, the availability of generators and network components were neglected [17]. There is significant uncertainty in renewable generation output and customer demand within an IM, which affects BESS optimal operation and sizing decisions. Neglecting or underestimating uncertainty could lead to violation of network constraints, whilst overestimating uncertainty or trying to deal with extreme cases could result in prohibitively high investment costs for the BESS [18]. Overestimating the reliability of the existing network could lead to the reliability benefits offered by the BESS being under-valued.

The existing sizing studies have used a variety of methods to model the impact of uncertainty. In Ref. [7], forecast errors for renewable generation, load, and electricity price are modelled and solved by robust optimization. Monte-Carlo simulation is applied in Ref. [19] to evaluate the sizing performance considering the uncertainty in generation and consumption. Reference [20] applies probabilistic unit commitment to address the uncertainty in wind farm production for BESS sizing. Stochastic programming is applied in Refs. [21,22] to account for the stochastic nature of renewable generation and load in a BESS sizing problem; A two-stage stochastic programming is applied in Ref. [23] to model the long term (cost development) and short term (load) uncertainties for optimal charging site design. Mean-variance Markowitz theory is applied in Ref. [24] to model the changes in microgrid cost when coupled by a BESS. A combined robust optimization with stochastic programming approach is applied in Ref. [25] to model the uncertainty arising from load, renewable generation, and charging/discharging efficiency. An expert fuzzy system-based approach is used in Ref. [26] to model the intermittency of renewable generation in sizing the BESS in an IM. Although the existing literature includes some methods which consider the effect of uncertainty on sizing study, they do not consider the impact of holding some of the BESS's power and energy resources in reserve to address uncertainty, which affects both its contribution to the system reliability and its income from markets and services. This relationship, which has not been considered in previous studies, can significantly affect the sizing results and system costs and is a key aspect of the method presented in this paper.

1.3. Novelty and contributions

The existing literature does not provide a comprehensive method for sizing BESS within IM that maximizes the business prospects, addresses uncertainty, and enhances system reliability while considering the interdependencies and potential conflicts and synergies between these goals. To fill this research gap, the present paper applies chance constrained programming (CCP) to optimally size a BESS in an IM with the objective of minimizing BESS lifetime cost; the reliability of the local network is included in the objective function as an expected cost of customer interruptions, quantified by EENS multiplied by Value of Lost Load (VOLL). The interdependencies between the goals are modelled using chance constraints, which are applied to the BESS state of charge, and are also used to calculate the unavailability of the BESS when evaluating system reliability. An optimal probability of chance constraint violation can be found, representing a compromise between revenue and reliability. The correlation between uncertain variables and battery degradation are modelled using Gaussian copula and a global wear coefficient, respectively.

Table 1 provides a comparative analysis of the features of the new model proposed in this paper and those considered in the literature. The inclusion of power flow equations renders the BESS sizing problem nonlinear and nonconvex. To ensure the tractability of the problem, this paper employs a state-of-the-art convex power flow model for radial networks using second-order conic programming (SOCP) [27]. This ensures a globally optimal and efficient solution using commercially available solvers.

The contributions of this paper are:

i) A comprehensive optimal sizing method for BESS in IM that accounts for the impact of capital and operational costs, income from ancillary services and energy trading, and IM reliability.
ii) The integration of a network reliability assessment method into the formal optimal BESS sizing problem formulation.
iii) A novel application of chance constraints to restrict the BESS's State of Charge in the presence of correlated uncertainty, which affects its ability to enhance system reliability through island-mode operation. This introduces the ability to identify an optimal trade-off between system reliability and investment and operation costs. The impact of the reliability of the wider network which supplies the IM and the value of lost load on this trade-off are investigated.

The rest of this paper is organized as follows: section 2 formulates the BESS sizing problem and presents the methodology. Sections 3 and 4 respectively describe a case study and analyze its results. Section 5 concludes the paper.

Table 1
Investigations of different features in sizing studies.

Key features	[10]	[12]	[13]	[14]	[15]	[19]	[7]	[8]	This paper
Uncertainty	✓			✓	✓	✓	✓		✓
Optimal power flow					✓		✓		✓
Convex optimization								✓	✓
Multi-service operation		✓	✓		✓	✓	✓		✓
Battery degradation			✓				✓	✓	✓
Island operation		✓	✓		✓		✓		✓
Uncertainty correlation									✓
Reliability as a constraint		✓	✓	✓					
Dependency between uncertainty and reliability	✓								✓
Dependency between reliability and profits					✓		✓		✓

2. Battery energy storage system sizing problem formulation and methodology

This section presents the optimal BESS sizing methodology. A flowchart of implementing the proposed sizing approach is presented in Fig. 1. Fig. 1 shows how the different methodological components are integrated to produce an overall methodology, as well as which subsections describe which components.

2.1. Deterministic battery energy storage system sizing problem formulation

This section describes the deterministic equations which are used to formulate the probabilistic sizing problem. For a given use-case, an optimal BESS size – in terms of power rating and energy capacity – can be found, which will minimize the cost of the BESS over its lifetime. The BESS sizing problem is resolved by minimizing the sum of the annualized operating cost, BESS capital cost (annualized by the discount factor and battery lifetime), and reliability cost subject to the IM's optimal operations over a representative simulation period. The deterministic BESS sizing problem is formulated as follows:

Subject to:

$$R_{\mathrm{FR}}(t) = A_{\mathrm{FR}}(t) \cdot P_{\mathrm{BESS}} \cdot T_{\mathrm{FR}} \tag{1b}$$

$$C_{RC} = EENS \cdot VOLL \tag{1c}$$

$$C_{\mathrm{El}}(t) = P_{\mathrm{G}}(t) \cdot \Delta t \cdot \Pi_{\mathrm{G}}(t) + \sum_{i=1}^{RG} P_{\mathrm{re},i}(t) \cdot \Delta t \cdot \Pi_{\mathrm{re},i}(t) \tag{1d}$$

$$BESS_{\mathrm{CC}} = C_{\mathrm{BESS}}^{\mathrm{en}} \cdot E_{\mathrm{BESS}} + C_{\mathrm{BESS}}^{\mathrm{pwr}} \cdot P_{\mathrm{BESS}} \tag{1e}$$

$$BESS_{\mathrm{LT}} \cdot \left(\frac{365}{D_{\mathrm{T}}} \cdot \sum_{t=1}^{T} (P_{\mathrm{ch}}(t) \cdot \Delta t \cdot \eta_{\mathrm{ch}} + P_{\mathrm{dis}}(t) \cdot \Delta t / \eta_{\mathrm{dis}}) \right) \cdot K_{\mathrm{w}} < 0.2 \cdot E_{\mathrm{BESS}} \tag{1f}$$

$$P_{\mathrm{net},i}(t) = -P_{\mathrm{ch,de}}(t) + P_{\mathrm{dis,de}}(t) - P_{\mathrm{L},i}(t) + P_{\mathrm{re},i}(t) \tag{1g}$$

$$Q_{\mathrm{net},i}(t) = -Q_{\mathrm{L},i}(t) + Q_{\mathrm{re},i}(t) \tag{1h}$$

$$\textit{Minimize } C_{\mathrm{Tot}} = \left(\frac{365}{D_T} \cdot \sum_{t=1}^{T} [C_{\mathrm{El}}(t) - R_{\mathrm{FR}}(t)] \right) + C_{RC} + BESS_{\mathrm{CC}} \cdot \frac{d(1+d)^{BESS_{\mathrm{LT}}}}{(1+d)^{BESS_{\mathrm{LT}}} - 1} \tag{1a}$$

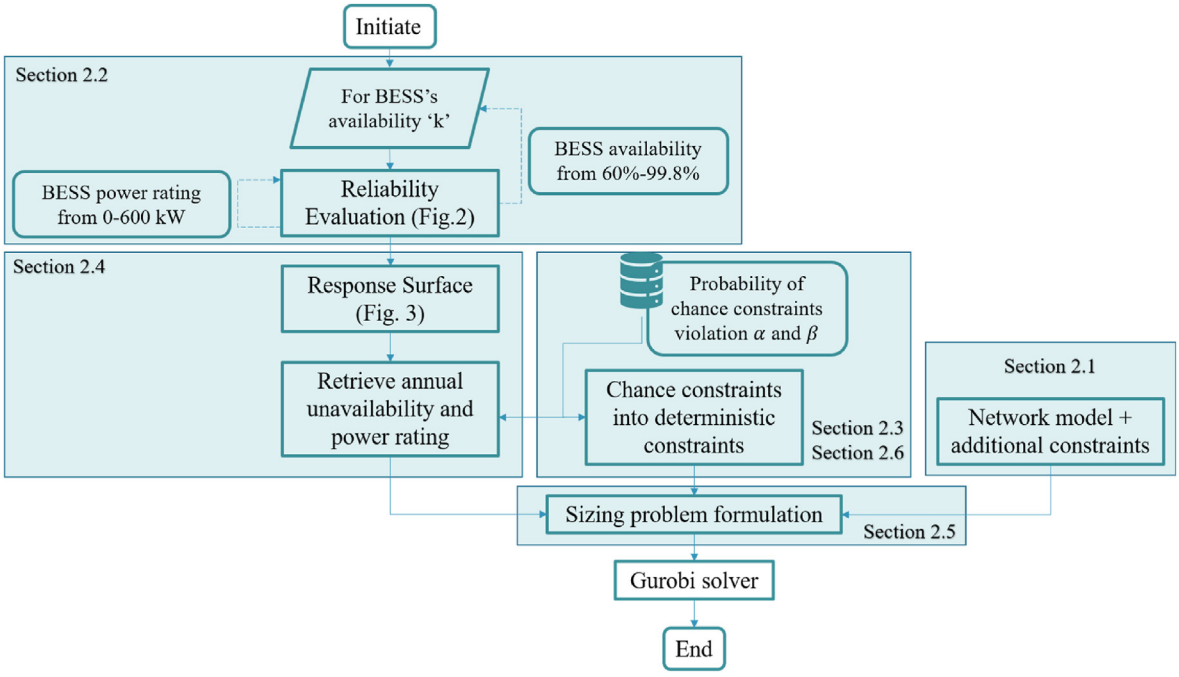

Fig. 1. Overall flowchart of implementing the proposed sizing approach. It describes (1) the IM system reliability evaluation given different BESS power rating and availability, (2) the integration of reliability evaluation within the CCP problem formulation, (3) the procedure of resolving the CCP.

$$P_{\text{net},i}(t) = \sqrt{2}G_{ii}u_i(t) + \sum_{\substack{k=1 \\ k\neq i}}^{N}[G_{ik}R_{ik}(t) + B_{ik}I_{ik}(t)] \tag{1i}$$

$$Q_{\text{net},i}(t) = -\sqrt{2}B_{ii}u_i(t) - \sum_{\substack{k=1 \\ k\neq i}}^{N}[B_{ik}R_{ik}(t) - G_{ik}I_{ik}(t)] \tag{1j}$$

$$2u_i(t)u_k(t) \geq R_{ik}^2(t) + I_{ik}^2(t) \tag{1k}$$

$$u_i(t) = V_i^2(t)\Big/\sqrt{2} \tag{1l}$$

$$R_{ik}(t) = V_i(t)V_k(t)cos(\theta_i(t) - \theta_k(t)) \tag{1m}$$

$$I_{ik}(t) = V_i(t)V_k(t)sin(\theta_i(t) - \theta_k(t)) \tag{1n}$$

$$E_{\text{b,de}}(t) = E_{\text{b,de}}(t-1) - E_{\text{b}}^{\text{stb}} + P_{\text{ch,de}}(t)\cdot\Delta t\cdot\eta_{\text{ch}} - P_{\text{dis,de}}(t)\cdot\Delta t\Big/\eta_{\text{dis}} \tag{1o}$$

$$BESS_{\text{CC}} \leq BESS_{\text{CC,max}} \tag{1p}$$

Equation (1a) represents the objective function of minimizing annualized BESS capital cost, operating cost, and reliability cost; (1 b) expresses the frequency response revenue, calculated as the product of the availability payment, the power rating of the BESS, and the number of hours committed to provide the ancillary service. (1c) calculates the system reliability cost, quantified by EENS multiplied by VOLL. (1 d) indicates the cost of importing electricity from the grid and renewable generators. (1e) is the calculation of battery capital cost. (1f) ensures the battery energy capacity is above 80% of its original capacity (an assumed end of life condition) at the end of the anticipated lifetime; K_{w} represents the relationship between battery degradation and usage, which offers an estimation of battery capacity fading considering the effect of operating Depth of Discharge (DOD); the calculation of K_{w} is based on [28] and summarized in Appendix B. Equations (1g) and (1h) restrict the active and reactive power balances. (1i) to (1n) are the convexification of complex power flow equations based on [27], the convexification is explained in detail in Appendix A. Equation (1°) shows the relationship between BESS state of energy and charging/discharging power. (1p) states that the investment spent on the BESS should be lower than the maximum available budget.

The evaluation of system reliability of (1c), in terms of EENS, is described in section 2.2. (1a) - (1 b), (1 d) - (1°) are formulated either in linear or second order conic form, which can be handled by off-the-shelf solvers.

2.2. System reliability evaluation

This section describes the reliability evaluation method which is used to link the optimal planning and sizing of the BESS to the reliability performance of the IM. In distribution networks, reliability indicates the ability to adequately supply demand with few interruptions over a long period [29]. The operational states of any system depend on the availability of the elements which comprise it, because failure of a component can shut down the entire system or leave it vulnerable to additional failures. Correct understanding and modelling of the failure probabilities for each element can be used to enumerate the likelihood of any operational state, and therefore the reliability of the system.

In this paper, the SMCS has been used to evaluate the annual reliability of the IM considering the probabilistic behavior of its elements. The application of Monte Carlo Simulation has been extensively addressed in the literature for the assessment of reliability indices of distribution networks [30]. SMCS generates an artificial operating history for the system which explores the different probability states; its sequential nature allows it to appropriately account for the time-dependent behavior of BESS, demand, and renewable generation, all of which are present in the case-study network.

The outage rate of network components, including branches, transformers, circuit-breakers, and fuses, can be modelled using a probabilistic approach, as can outages of supply from the wider network, which are aggregated at the point of common coupling (PCC) with the IM [31]. The simulated outage history for each element within the system can be randomly generated by calculating the 'Up' and 'Down' state sequence for the simulation period by using the Mean Time To Failure (MTTF) and Mean Time To Repair (MTTR) [32] of the components and applying Eqs. (2) and (3):

$$Up_{time} = -MTTF\cdot\ln(U_1) \tag{2}$$

$$Down_{time} = -MTTR\cdot\ln(U_2) \tag{3}$$

where U_1 and U_2 are uniformly distributed random numbers between 0 and 1.

During grid-connected operation of the IM, the BESS can charge or discharge depending on the demand, power, and operational scheduling. However, enough energy needs to be held to manage the IM frequency and voltage during power island operation, so the SoC needs to remain within some limits.

To reproduce such operational characteristics, the BESS was modelled using two variables: BESS availability, $BESS_A$, and its discharging state, $BESS_{DS}$. The first term aggregates the intrinsic availability of its components and the probability of the battery being within 10%–90% of SOC and is linked to the chance constraints as discussed in section 2.4. Higher $BESS_A$ values mean the BESS is more likely to be able to support the IM in post-fault island operation. The second variable simulates the battery's scheduling process, where an "Up" state means a charging period and lower values indicate a higher probability of the battery being either discharging or idle. The BESS can then be integrated into the MCS using Eqs. (2) and (3).

The power output from distributed generators and load demand vary with daily, weekly, and yearly seasonalities. By using historical data for demand and generation in combination with component's availabilities, the overall stochastic characteristics of the IM can be modelled within the MCS.

The reliability indices for each load point, k, were calculated based on analysis of the outage history of the network elements between the load point and the generators. For a radial system and considering the generator m as the source of energy, these can be assessed by

$$\lambda_k^m = \sum_i \lambda_i [failures\ /\ year] \tag{4}$$

$$U_k^m = \sum_i \lambda_i \cdot r_i [hours\ /\ year] \tag{5}$$

$$r_k^m = \frac{U_k}{\lambda_k}[hours] \tag{6}$$

where λ_i, U_i and r_i stands for the outage rate, annual supply unavailability and outage duration time of the element i (elements are circuit sections or transformers).

Each load can be supplied by either the PCC, or the BESS and local generation. After calculating the reliability indices for load point k for each available generator using Equations (4)–(6), the load point unavailability can be assessed by aggregating the contributions from each source, considering the upstream network, distributed sources and BESS

$$U_k = \prod_m U_k^m \cdot U_s \cdot U_{BESS} \tag{7}$$

where U_k^m is the annual supply unavailability of load point k related to generator m; U_{BESS} and U_s represent the battery and the upstream network's annual unavailability. The latter is modelled based on typical SAIDI (System Average Interruption Duration Index) and CAIDI (Consumer Average Interruption Duration Index) indices from distribution networks. The SAIDI and CAIDI can be translated to the network's annual unavailability and repair time, respectively.

For each timestep in the MCS, a Generation Adequacy evaluation step is performed. At this step, based on the DER's power output, the ratio between power imbalance and battery's power rating is calculated to evaluate the system's capability to maintain island mode operation. The load point's unavailability is updated whenever the power imbalance cannot be met, which is followed by a demand response or load shedding scheme until the load demand is fully supplied by the sources.

Reliability is quantified using the EENS index. For each load point, k, the EENS can be calculated by

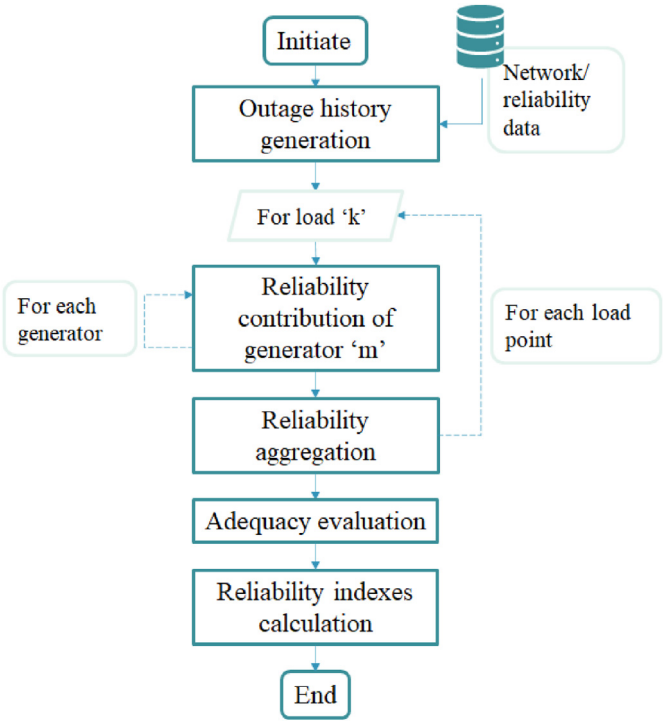

Fig. 2. General reliability evaluation considering multiple feeding paths and generation adequacy.

$$EENS_k = U_k \cdot L_k[MWh/year] \tag{8}$$

where L_k is the mean active power demand for load point. k.

Hence, the EENS for the whole system can be calculated by

$$EENS = \sum_k EENS_k \tag{9}$$

A flowchart outlining the reliability assessment methodology is shown in Fig. 2.

2.3. Application of chance constraints

CCP has been widely applied in solving power system operation and planning problems, as for example in Refs. [33,34], respectively. A chance constraint – which can be violated with a specified probability – can be used to introduce uncertainty into an otherwise deterministic optimization problem. In solving the optimal planning problem, the application of CCP allows avoiding over investment in BESS capacity to accommodate extreme cases with near-zero probability, enabling a compromise between economically sizing of the BESS and accounting for operation under uncertainty; the probability of violating the chance constraints can be specified by the user, allowing their attitude to risk to be included in the analysis.

In this paper, it is assumed that the IM can disconnect from the main distribution network and operate as an island. One of the BESS's functions is to address load imbalance within the IM, including those arising from demand and generation uncertainty, to keep the system operable during island mode operation or delivering to its optimal schedule in grid-connected mode. Consequently, the probability of the BESS reaching its state of charge limits is a function of the uncertainty in demand and generation – represented by the probability distribution of the forecast errors for these values. The forecasts are not independent, and correlations between forecast errors are modelled by Gaussian copula, formulating a joint distribution, as explained in Appendix C. The uncertain demand forecast errors are modelled in this paper, but the method would be valid for uncertain generation forecasts or forecasts of both demand and generation.

The forecasting error $\xi_{e,i}$ can be included in (1g) by substituting the active power demand $P_{L,i}$ with the sum of the forecasted demand $P_{LF,i}$ and forecasting error $\xi_{e,i}$

$$P_{net,i}(t) = -\tilde{P}_{ch}(t) + \tilde{P}_{dis}(t) - P_{LF,i}(t) - \xi_{e,i}(t) + P_{re,i}(t) \tag{10}$$

The decision variables and constraints in (1) which relate to the BESS are converted to stochastic variables and constraints due to the inclusion of forecasting error, $\xi_{e,i}$. In this paper, it is assumed that the BESS alone addresses the effect of uncertain load forecast errors. Therefore, only the BESS-related variables and constraints are stochastic, other decision variables and constraints remain deterministic.

Linear decision rules (LDRs) [35] are applied to handle the stochastic equality constraints and reduce the number of stochastic variables to make the problem tractable. LDRs define affine policies which allocate uncertainty to each respective party that addresses its impact. In this paper, LDRs assign the responsibility of addressing uncertain forecast errors to the BESS according to (11a) - (11c):

$$\tilde{P}_{ch}(t) = P_{ch,de}(t) + W_{ch}(t) \cdot \xi_{e,s}(t) \tag{11a}$$

$$\tilde{P}_{\mathrm{dis}}(t) = P_{\mathrm{dis,de}}(t) + W_{dis}(t)\cdot\xi_{\mathrm{e,s}}(t) \tag{11b}$$

$$W_{dis}(t) - W_{ch}(t) = 1 \tag{11c}$$

$$P_{\mathrm{net},i}(t) = -P_{\mathrm{ch,de}}(t) + P_{\mathrm{dis,de}}(t) - P_{\mathrm{LF},i}(t) + P_{\mathrm{re},i}(t) \tag{11d}$$

As (11a) and (11 b) show, the stochastic battery charging and discharging power vales are expressed as a deterministic variable plus the sum of uncertain load forecast errors multiplied by a weighting factor. The weighting factor represents the proportion of uncertainty affecting or offset by the relevant stochastic variable, and (11c) means the BESS charge or discharge to offset the impact of uncertainty. Consequently, the balance between deterministic variables can be obtained as (11 d).

The BESS operates to balance the system and offset forecast errors at each bus based on the LDRs (11a) and (11 b), which assume that the forecast errors can be aggregated at the bus with BESS. The influence of load forecast errors on other parameters of the IM, such as the bus voltage and flow loss are assumed small, and their duration of these errors are short, allowing them to be safely be neglected.

Because the BESS operates to address the aggregated load forecast error $\xi_{\mathrm{e,s}}$, (1°) is modified to (12) and (13):

$$\tilde{E}_{\mathrm{b}}(t) = \tilde{E}_{\mathrm{b}}(t-1) - E_{\mathrm{b}}^{\mathrm{stb}} + P_{\mathrm{ch,de}}(t)\cdot\Delta t\cdot\eta_{\mathrm{ch}} - \frac{P_{\mathrm{dis,de}}(t)\cdot\Delta t}{\eta_{\mathrm{dis}}} - \xi_{\mathrm{e,s}}(t)\cdot\eta_{\mathrm{er}}(t) \tag{12}$$

$$\eta_{\mathrm{er}}(t) = \begin{cases} \eta_{\mathrm{ch}}, & if\ \xi_{\mathrm{e,s}}(t) \le 0 \\ \dfrac{1}{\eta_{\mathrm{dis}}}, & if \xi_{\mathrm{e,s}}(t) > 0 \end{cases} \tag{13}$$

where η_{er} causes the battery to charge or discharge in response to the load forecast errors. The BESS at one time step should be able to address the impact of uncertainty in previous time steps, which introduces the constraint as:

$$\tilde{E}_{\mathrm{b}}(t) = E_{\mathrm{b,de}}(t) - \sum_{\widehat{t}=1}^{t} \xi_{\mathrm{e,s}}(\widehat{t})\cdot\eta_{\mathrm{er}}(\widehat{t}) \tag{14}$$

This indicates that the impact of uncertain variables on battery operation accumulates with time, hence the reserve kept in the battery to address the uncertainty is increasing with the duration of the analyzed time window (D_T in (1a)). Because addressing the accumulated uncertainty limits BESS's capacity to provide other services, or the available budget may fail to render a large enough battery capacity to accommodate the accumulated forecast errors. To avoid this, this paper assumes the forecast error will accumulate for the 95th percentile of reversal time of the forecast error.

Based on (14), the deterministic variable of battery state of energy $E_{\mathrm{b,de}}(t)$ can therefore be expressed as:

$$E_{\mathrm{b,de}}(t) = E_{\mathrm{b,de}}(t-1) + P_{\mathrm{ch,de}}(t)\cdot\Delta t\cdot\eta_{\mathrm{ch}} - \frac{P_{\mathrm{dis,de}}(t)\cdot\Delta t}{\eta_{\mathrm{dis}}} \tag{15}$$

$E_{\mathrm{b,de}}$ is constrained by the battery capacity E_{BESS}, which is expressed as

$$0 \le E_{\mathrm{b,de}}(t) \le E_{\mathrm{BESS}} \tag{16}$$

The stochastic battery state of energy $E_{\mathrm{b}}(t)$ is formulated using chance constraints due to the inclusion of uncertain load forecast errors; these are formulated as

$$\Pr(\tilde{E}_{\mathrm{b}}(t) \le 0) \le \alpha \tag{17}$$

$$\Pr(\tilde{E}_{\mathrm{b}}(t) \ge E_{\mathrm{BESS}}) \le \beta \tag{18}$$

Pr in (17) and (18) indicate the probability that the constraint is not violated, and α and β are the highest acceptable probabilities with which the constraints can be violated. In this case, the battery is permitted to reach its upper or lower state of charge constraints with known probabilities. The inclusion of chance constraints avoids unnecessarily high investment in battery capacity to accommodate extreme cases of load forecast error. Higher values for α and β will lead to more of the BESS's resources being committed to revenue-oriented functions such as frequency response and energy trading; this will increase the likelihood that the BESS reaches its SoC limit when managing the demand forecast errors, and therefore becoming unable to facilitate island mode operation.

2.4. Chance constraints and battery energy storage system availability

The BESS has a crucial role in maintaining the local system's operational state by correcting local imbalances to maintain the frequency and voltage during island mode operation. In these circumstances, the battery power rating, capacity, and operating schedule have a major impact on the network's reliability indices. The power rating affects the capability of the BESS to manage the power imbalances, whilst the battery capacity is associated with the availability of energy within the BESS.

The reliability evaluation method described in Section 2.2 is used to quantify the relationship between the BESS availability and power rating and the unavailability of the IM. For a case study network, this is done by evaluating the unavailability of the island microgrid for feasible combinations of BESS availability and power ratings. For the case study used in this paper, the availability was examined from 60% to 98% in steps of 2% and the BESS power rating from 50 to 600 kW in steps of 50 kW. Fig. 3 depicts the resulting relationship between the battery's availability, power rating and the network's annual unavailability (the number of hours per year that the network is unable to operate due to a concurrent loss of supply from the PCC and BESS). It illustrates the significant influence of both the battery's availability and power rating on the network's annual unavailability, showing a better chance of maintaining the system in operation at high availability levels.

The sum of the chance constraint probabilities (α+β) is the probability of constraint violation (PoCV). As discussed in section 2.3, probability levels α and β are applied to restrict the operating boundary of the BESS. The value of 1-(α+β) is used as an estimate of the BESS battery availability (explained in section 2.2) for the reliability evaluation; this is because if the battery has reached its upper or lower SOC boundary, it will no longer be able to provide frequency response in islanded operation, and customer supplies will be disconnected. This results in a relationship between the probability level of the chance constraints and the annual unavailability of each load bus; the impact of this on the IM as a whole is shown in Fig. 3. The BESS power rating affects its ability to offset power imbalance, and thereby affects the unavailability of customer supplies. Piecewise linear functions were used to estimate the relation between BESS power rating and annual unavailability when the value falls between the values for which the reliability evaluation method was used, this relationship f_{pw} is expressed as:

$$U_k = f_{pw}(\alpha, \beta, P_{BESS}) \tag{19}$$

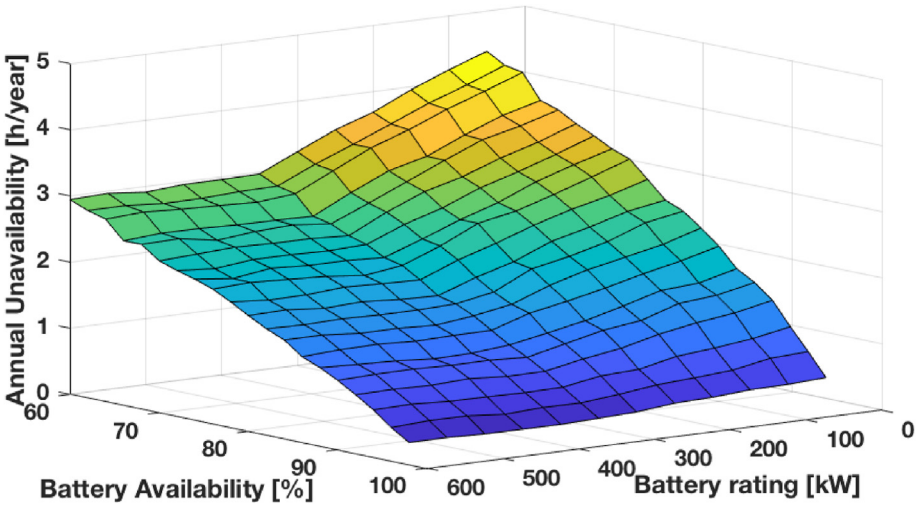

Fig. 3. Relation between network annual unavailability, battery rating (50–600 kW), and battery availability (60%–98%).

The annual unavailability is then be applied to calculate the EENS according to (8)–(9). This allows the complex, non-linear reliability evaluation to be integrated into the optimization problem as a set of linear functions.

2.5. Chance-Constrained Programming problem formulation for battery sizing

Overall the CCP problem is formulated as:
Minimize (1a).
Subject to: (1 b) - (1n), (8), (9), (11c), (11 d), (13)–(19).
Solving the CCP problem means finding the optimal deterministic decision variables (as listed in Nomenclature) which satisfy the system constraints and chance constraints, under the condition that the uncertain variables are distributed according to their joint distribution.

2.6. Transformation of chance constraints

The CCP problem cannot be directly solved by a conventional optimization approach due to the probabilistic chance constraints (17) and (18). This is dealt with by transforming the chance constraints to deterministic constraints, while ensuring the optimization problem can still be formulated as a convex problem. Equations (17) and (18) can be converted to (20) and (21) based on (14),

$$\sum_{\widehat{t}=1}^{t} q_{\xi_{e,s}(\widehat{t})}(1-\alpha)\cdot\eta_{er}(\widehat{t}) \le E_{b,de}(t) \tag{20}$$

$$\sum_{\widehat{t}=1}^{t} q_{\xi_{e,s}(\widehat{t})}(\beta)\cdot\eta_{er}(\widehat{t}) \ge E_{b,de}(t) - E_{BESS} \tag{21}$$

because the quantile of uncertain variables follows a monotonic relationship with its inverse cumulative distribution function. The quantile q is defined as the inverse function of the load forecasting error's cumulative distribution function (CDF) with the probabilities α and β. The quantiles can be derived if the joint distribution of load forecast errors is known.

In this paper, Gaussian copula is applied to capture the correlations and generate correlated samples; MCS is then used to derive the CDF of the uncertain term $\xi_{e,s}\cdot\eta_{er}(t)$ in (12); based on the correlated samples, the quantile can then be derived from the CDF with a given probability.

For example, the BESS investigated in the Case Study addresses the correlated forecast errors at six buses. The probability distribution function (PDF) of the aggregated forecast errors at time step 1 and related CDF are shown in Fig. 4(a) and (b). If α and β are 5%, the related quantile values of $\xi_{e,s}\cdot\eta_{er}(t)$ are calculated as 0.032 MWh and −0.0285 MWh. It can also be observed from Fig. 4(a) that the results from CCP can address 90% of uncertain load forecast errors, the 5% extreme cases of power redundancy because of the forecast errors in [−6.76%,-3%] can be discarded, and the power shortage due to the forecast error in [3%,7.73%] can be resolved by extra import from the local renewable generators or grid in a real-world application.

By implementing this method, chance constraints (17) and (18) can be essentially converted to linear constraints, hence the stochastic CCP optimal sizing problem is reformulated as a deterministic convex problem. The BESS needs to reserve enough energy to cover the uncertainties, which effectively reduces its useable capacity; this means the minimum SoC constraint will be greater than the true minimum SoC and the maximum SoC constraint will be less than the true maximum SoC.

3. Case study description

This section introduces the case study in terms of the summary of Gussing distribution network for demonstration, IM use cases identified in the MERLON project, and specification of each scenario in case study.

3.1. Summary of distribution system

The case study for this paper is the Gussing distribution network shown in Fig. 5, with the Strem area, which will act as an IM, clearly identified. This is a real-world 20 kV distribution network in Austria and is one of the demonstration sites for the H2020 MERLON project [36]. The SOCP-based CCP for sizing the battery is formulated in Matlab 2019a and solved by Gurobi [37].

As shown in Fig. 5, the Güssing distribution system is connected to the wider distribution network by an incoming feeder connected to bus T304. Buses T265 and T267 are connected via a switch which is open during normal (pre-fault) operation, but can be closed to provide an alternative supply to either feeder. Renewable

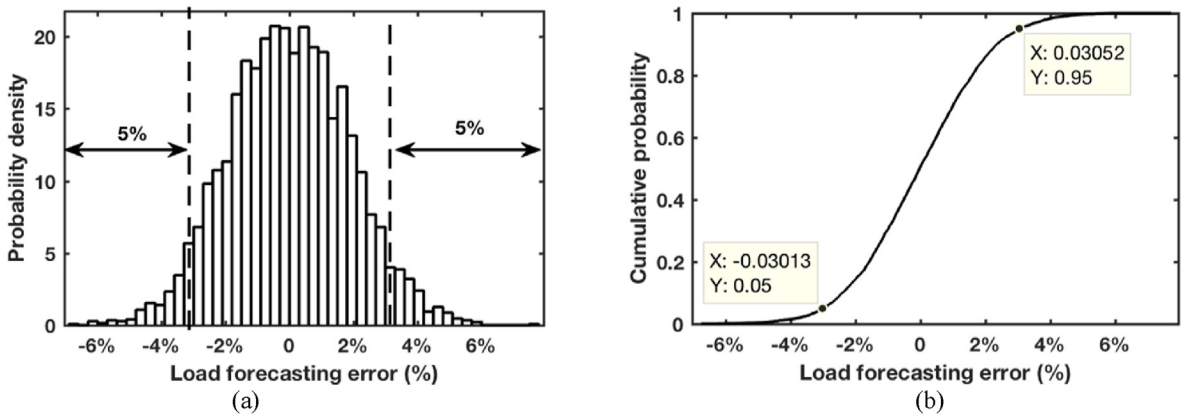

Fig. 4. PDF (a) and CDF (b) of aggregated load forecast errors of Merlon IM at time step 1, which label the 5% extreme cases on both sides.

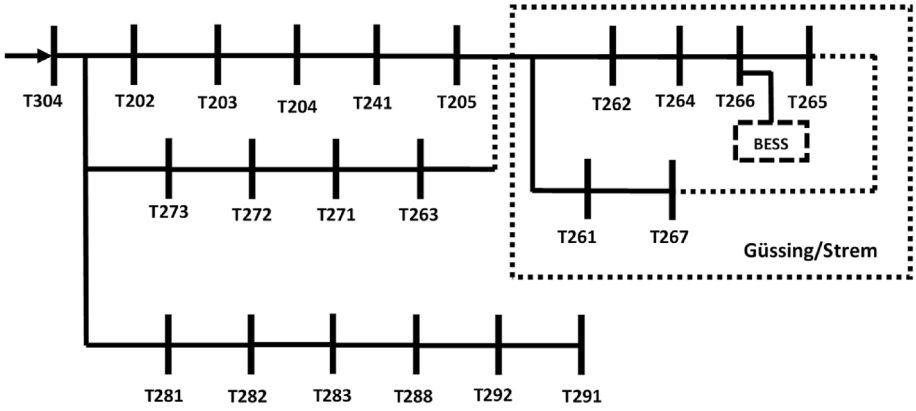

Fig. 5. 20-kV Güssing distribution system with the feeder connecting to bus T304. The Strem area in the top-right of the figure is the local area which will form the IM.

generators and electricity users, including public and residential buildings, are connected to the network. The Strem area that acts as the IM can be disconnected from the rest of the Güssing network and operate in island mode in response to system requirements or faults; this is enabled by the BESS which is connected at bus T266.

3.2. Island microgrid use cases

The business use cases of the IM and BESS within the MERLON project [36] are:

- Local distribution grid management to address the voltage and power flow operation constraints. For example, the analyzed Austrian distribution system in this paper has a strict restriction on voltage limitations of ±2% of the nominal value [38].
- Provision of secure supply during island mode operation: to improve the system reliability considering possible disconnection between the IM and grid.
- Participation in energy markets: the BESS is assumed to respond to variations in the wholesale electricity price between 06:00−00:00 every day in this study.
- Provision of balancing services to the Transmission System Operator (TSO): the BESS is designed to join the Austrian balancing market to provide Frequency Containment Reserves (FCR), which is automatically activated within 30 s upon request [39]; it is assumed in this study that the BESS maintains its State of Charge between 40% and 60% in 00:00−06:00 to allow it to respond to FCR requests. The BESS receives an availability payment for providing this service.

3.3. Case study specification

Four scenarios are investigated in case study, and they are explained as follows:

i) Scenario 1: Investigating the effect of different chance constraint probability levels on the proposed sizing study.
ii) Scenario 2: Investigating the impact of neglecting uncertainty within the sizing study.
iii) Scenario 3: Investigating the impact of battery lifetime and degradation.
iv) Scenario 4: Investigating the relationship between optimal battery size, value of lost load, and system reliability.

The input parameters applied in the case study are shown in Table 2; the availability payment for providing frequency response is taken from Ref. [39]. The BESS is assumed to charge or discharge with maximum power in the event of primary frequency response, which is (based on analysis of historical data) required 7 times between 00:00 to 6:00 a.m. [40]. Electricity demand of eight representative days, comprising a weekday and a weekend day of each season, were selected for implementing the sizing study, with a time step of 1 h. Fig. 6 shows the load demand at one bus in the case study network for the eight representative days, where the demand in summer and autumn (time step 49 to 145) is lower than

Table 2
Parameters for the sizing problem.

BESS parameters	
Capacity unit cost	316 €/kWh
Power rating unit cost	200 €/kW
$BESS_{CC,max}$	200,000 €
Charging/discharging efficiency	95%
Operating limits	0 ≤ SOC ≤100%
VOLL	30,000 €/MWh
Lifetime	15 years
Discount rate	6%
95th percentile of forecast error reversal time	5 h
Frequency response	
Availability payments	22.01 €/MW/h

the demand in winter and spring. The distributions of the uncertain load forecast errors for each of the 8 days was obtained by fitting appropriate subsets of historical data over one year depending on day of the week and season with Guassian copula; the correlation between demand at two buses in Strem can be observed in Fig. A1. The maximum available buget for the BESS was €200,000.

For the reliability modelling, the failure of the main incoming supply to the network was calculated using the expected SAIDI and CAIDI. The historical demand and generation data, branch parameters, SAIDI and CAIDI were provided by the Distribution System Operator (DSO), Energie Güssing. The data in Table 2 represent a base case, and the impact of varying of these parameters is investigated in the test-case scenarios.

4. Case study results and discussion

This section presents the results from each scenario and discussions.

4.1. Scenario 1

Scenario 1 investigates how setting the chance constraints to different probability levels – which reflects the operator's attitude to risk – affects the optimal battery sizing. Sensitivity analysis is performed by applying the proposed battery sizing framework with different probabilities varying from 20% to 0.1%. As the PoCV increases, the cost of operating the system falls, the BESS power capacity increases and the BESS energy capacity reduces; however, the system reliability cost increases. For a given PoCV, the sum of the system and reliability costs will be a minimum; this PoCV represents an optimal trade-off between system profits and reliability.

The optimal BESS capacity and power rating corresponding to each chance constraint probability levels are shown in Fig. 7. The optimal battery configuration stays idle with 0.295 MWh and 0.533 MW when the PoCV is higher than 18.8%; the optimal capacity gradually increases from 0.295 MWh to 0.575 MWh with the PoCV reduces from 18.8% to 1.1%; the optimal battery power rating accordingly decreases from 0.533 MW to 0.092 MW. The CCP fails to find a feasible solution when PoCV is lower than 1.1%, since the load forecast errors cannot be addressed in some extreme cases due to the limited budget (200,000€).

Fig. 8 shows the trade-off between reliability and cost as the PoCV varies. The reliability cost C_{RC} in (1c) is depicted by the orange line in Fig. 8(a) and the blue line indicates the sum of annualized battery capital cost and electricity cost minus the revenue from providing frequency response. Fig. 8(b) shows the total system cost C_{Tot} as in (1a), which is reached by summing the two lines in Fig. 8(a). As shown in Fig. 7, the reduction of PoCV leads to an increase in BESS capacity; the BESS power rating is reduced due to the limited budget. Changing BESS size leads to reduced income from providing frequency response according to (1 b), hence the blue line in Fig. 8(a) trends to increase.

Lower PoCV indicates a higher battery availability, and consequently a decrease in EENS; the reliability cost is therefore decreased as shown in Fig. 8(a). Fig. 8 indicates that a trade-off can be reached between IM reliability and revenue to pursue the optimized overall system cost. In this case, the minimum total cost is reached when the PoCV is 5.8%.

4.2. Scenario 2

This scenario compares the proposed sizing approach with the method presented in Ref. [13], in which the impact of uncertainty has been neglected. The sizing study excluding uncertainty at the planning stage yields an optimal battery configuration of 0.295 MWh and 0.533 MW. This was derived with a PoCV of 18.8%, it represents the point at which the battery size stopped changing as the PoCV was increased (see Fig. 7) and is the design which would be obtained if the uncertain variables were modelled as deterministic. The related annualized system cost could be reduced by €11,429 compared with the optimal trade-off point from Fig. 8 due to the greater revenue from frequency response provision enabled by a higher power rating. The payback period can be reduced from 11.50 years to 6.94 years if only the revenue of

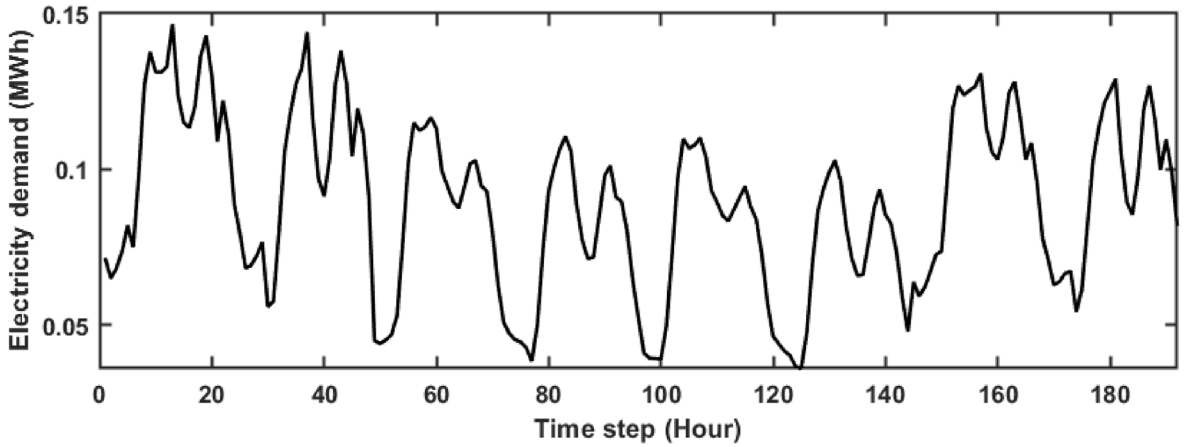

Fig. 6. Electricity demand of one bus in Strem over 8 representative days, each hour is a time step.

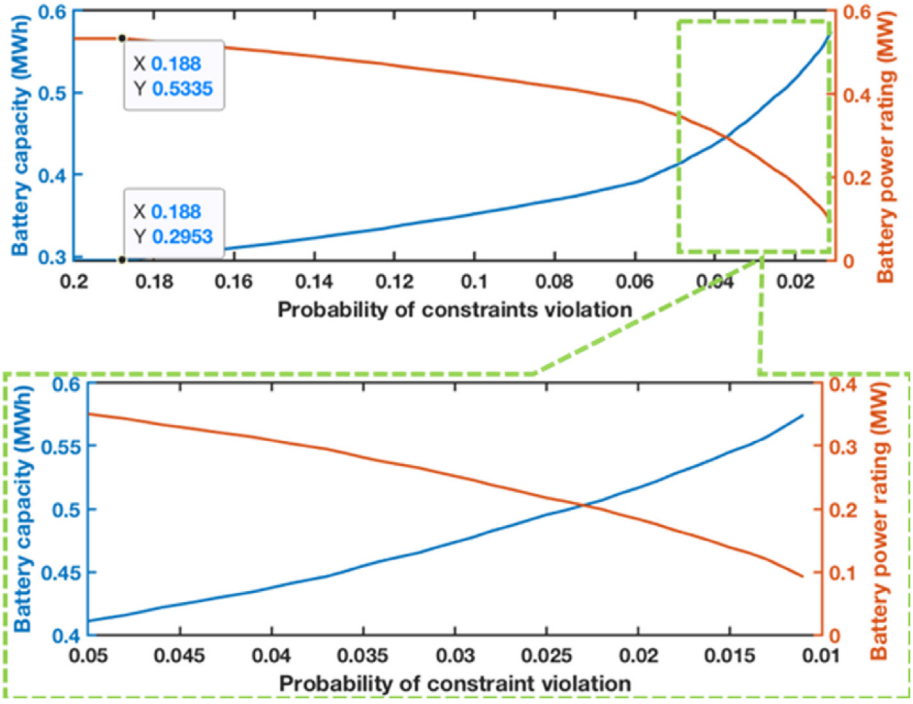

Fig. 7. Optimal BESS capacity (blue) and power rating (orange) against PoCV changing from 20% to 1.1%.

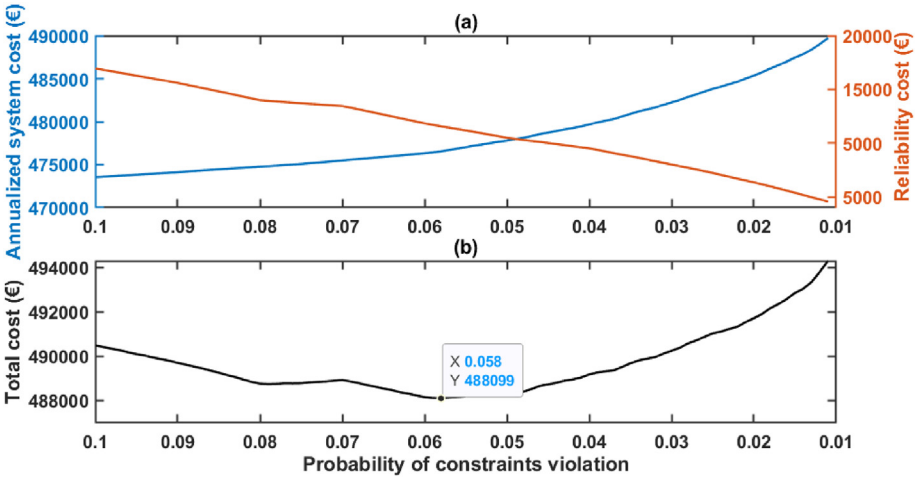

Fig. 8. Costs against different PoCV changing from 10% to 1.1%. (a) Sum of annualized BESS capacity cost and operating cost (blue) and reliability cost (red) against different PoCV. (b) Total system cost, derived by adding the two lines in (a).

arbitrage and providing frequency response are considered. However, this also corresponds to a battery availability for post-fault islanding of 62.4%, leading to an absolute EENS of 1.224 MWh with a correspondingly higher reliability cost of €36,720. This higher cost shows the reduction in system reliability if uncertainty is neglected, which is far from the optimal trade-off between reliability and cost observed in Fig. 8.

4.3. Scenario 3

The annualized total costs, i.e. C_{Tot} in (1a), against different lengths of anticipated BESS lifetime are shown in Fig. 9, where the blue line indicates the sizing results considering battery degradation, and the orange line is for the results excluding the impact of battery degradation. As seen, the annualized total cost decreases with the increase of anticipated lifetime for using the BESS, this is because that an increase of battery lifetime would reduce the annualized BESS capital cost. Additionally, the difference between the two curves increases when the BESS anticipated lifetime increases. Because according to (1f), BESS is only capable of providing limited quantity of energy before reaching its end of life, hence the high revenue of frequency response provision would be preferred rather than arbitrage, and less capacity would be allocated for arbitrage with the increase of anticipated battery lifetime; on the other hand BESS can be frequently charged and discharged to provide both frequency response and arbitrage when the impact of battery degradation is not considered, leading to increased revenue and hence reduced overall cost.

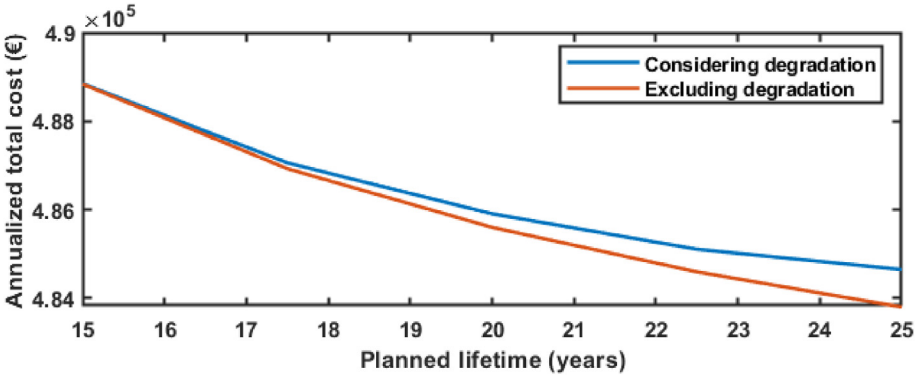

Fig. 9. Annualized total costs considering the impact of battery degradation (blue) and excluding the degradation factor (orange) against planned lifetime for using BESS.

The optimal battery configurations derived from both the cases of considering and excluding battery degradation are the same. However, for a sizing study with higher available investment, the exclusion of battery degradation impact could result in a trade-off point higher than the optimal PoCV from the case of considering battery degradation; this is because that a higher revenue could be gained from unlimited charging and discharging for arbitrage and when the battery capacity is larger because of higher investment, the annualized system cost as in Fig. 8(a) would be lower, and the trade-off point would therefore be higher than the optimal PoCV from considering battery degradation.

4.4. Scenario 4

The VOLL reflects the willingness of consumers to invest to improve their supply reliability [41]. As the VOLL increases, the customers are less willing to tolerate an interruption in supply and therefore more willing to invest in system reliability through their energy bills. This scenario investigates the impact of VOLL on battery sizing, and on the optimal trade-off between system cost and reliability represented by the PoCV. The optimal BESS size and probability of constraints violation corresponding to different values of VOLLs, are shown in Fig. 10.

As the VOLL increases, the best PoCV for reaching a trade-off between system reliability and revenue decreases, consequently the BESS capacity increases, and the power rating decreases. This indicates that consumers require higher battery availability to improve reliability, which reduces the income generated by providing frequency response. The VOLL of private end users are generally between 10,000 and 50,000 €/MWh [41], the optimized battery capacity and power rating respectively increase from 0.295 MWh to 0.415 MWh and decrease from 0.533 MW to 0.343 MW when the VOLL changes from 10,000 to 50,000€/MWh; the optimized PoCV varies from 18.7% to 4.8% to reach the optimal balance between reliability and cost. Industrial and commercial users have higher requirement for system reliability, with VOLL increasing to as much as 150,000 €/MWh [41]. The optimal PoCV slightly increases from 1.4% to 1.2% when the VOLL ranges from 70,000 to 100,000, and remains at 1.1% when the VOLL is 110,000 or higher.

Based on the analysis of historical data, the main incoming supply to the Güssing distribution system has an availability of 99.89%. By taking this as the base scenario, two other comparative scenarios are developed with the availability of power source being 99.97% and 99.02%. The optimal PoCV for VOLLs from 10,000 to 150,000 €/MWh for the three availability scenarios are depicted in Fig. 11. When the incoming supply has a high availability of 99.97%, the optimal PoCV remains close to 20% for VOLLs up to 50,000 €/MWh; the optimal PoCV is 1.1% for all levels of VOLL when the incoming supply availability falls to 99.02%. The results indicate that there is no trade-off point between system cost and reliability in implementing the sizing study for a distribution system with availability of 99% or lower: the BESS with the highest availability is always pursued to improve the IM reliability; conversely, the BESS is not necessary to maintain at a high availability to improve system reliability if the distribution system is highly-reliable, instead, a lower availability but with higher power rating can be obtained to improve the revenue for providing ancillary services, hence various trade-off points can be observed with different VOLLs.

5. Limitations and future work

The proposed sizing approach benefits the system operator and project investors with maximized improved network performance

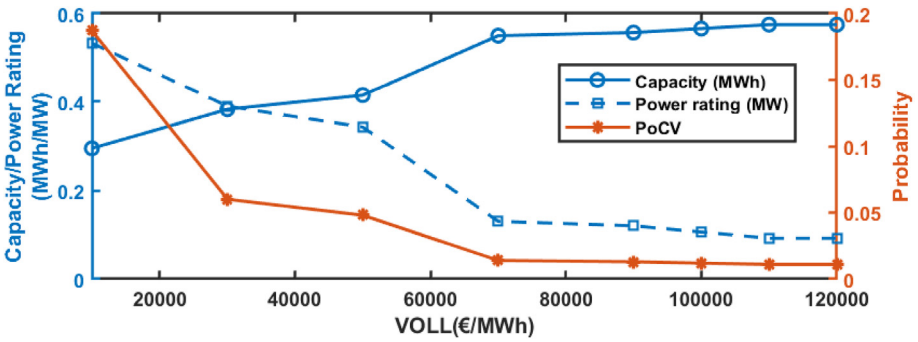

Fig. 10. Battery sizing results in terms of capacity (blue solid line with circles), power rating (blue dashed line with squares), optimal PoCV (orange line) with different VOLL.

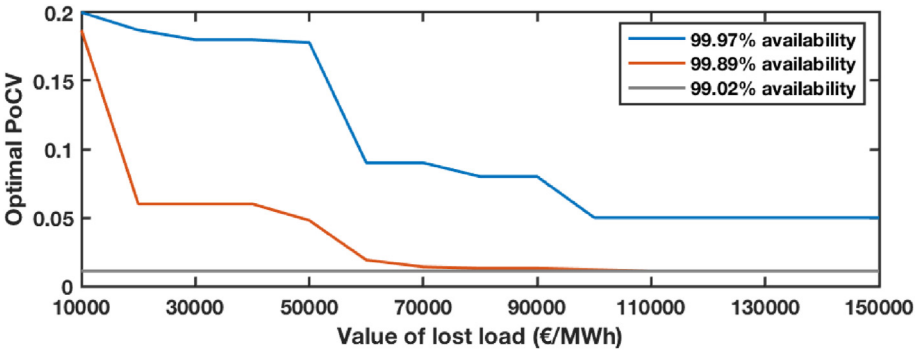

Fig. 11. Optimal PoCV against different VOLL changing from 10,000 to 150,000, the blue, orange, and grey lines respectively represent the optimal PoCV with 99.99%, 99.89%, 99.02% of availability of incoming supply.

and good returns on investment. The work can be further extended by the following research perspectives:

i) How the DSO should remunerate the BESS owners for providing this service is a vital topic, and one which will be investigated via the generation of new business models within the MERLON project.
ii) The model proposed in this paper can be expanded for sizing a BESS to fulfil other services such as peak shaving and capacity firming, and with more complicated complex uncertainties in a distribution system.
iii) A sizing scheme for Island Microgrids, considering the integration of multiple energy vectors, can be investigated.
iv) In this paper, capacity fade is modelled only as a function of operating Depth of Discharge; this could be extended by considering the degradation factor of lifetime throughput, inspired by Ref. [23].

6. Conclusion

This paper proposes the use of Chance-Constrained Programming to compute the optimal size of a BESS in an Island Microgrid (IM) with the objectives of minimizing system cost and improving reliability. The chance constraints are applied in a novel way which represents the availability of the BESS to improve reliability during an islanding event. The main findings can be summarized as follows:

- It is essential to consider the probability that the BESS will be available to provide a secure supply to the IM in the event of a fault on the wider network; increasing this probability will reduce the income the system can obtain via energy and ancillary service markets, but may maximize the overall value of the BESS, particularly if the local distribution network is unreliable.
- The sizing problem for a realistic primary distribution network, with an IM comprising several buses, can be efficiently solved by this method. If the distribution system supports private end users with a VOLL of 50,000€/MWh, an optimal 4.8% of probability of constraints violation is found to balance the system reliability and operating cost, highlighting the trade-off between them. The optimal size of the battery is 0.415 MWh with 0.343 MW. As a comparison, the optimal size of the battery is 0.295 MWh with 0.533 MW if the uncertainty is not considered within the sizing problem, this would lead to more income from ancillary service markets but would reduce the system reliability to unacceptable 18.8% of PoCV and would result in a non-optimal trade-off because the uncertainty was neglected.
- The optimal probability of constraints violation decreases when the consumers' willingness to maintain system reliability, i.e., VOLL, is increased. A lower PoCV, corresponding to a BESS with higher availability, is also required in a less-reliable distribution system.
- When batter degradation was excluded from the sizing study, it led to a higher optimal PoCV value than in the case which included degradation. The corresponding battery configuration would compromise IM reliability, with an overall higher total cost to system operator.

The proposed SOCP-based CCP benefits the system operator and project investors by allowing them to maximize the benefits of a BESS fulfilling multiple, conflicting objectives in the face of uncertainty.

Author statement

Da Huo: Conceptualization, Methodology, Formal analysis, Software, Writing – original draft, Writing – review & editing; **Marcos Santos**: Methodology, Software; **Ilias Sarantakos**: Methodology, Formal analysis, Writing – review & editing; **Markus Resch**: Resources, Data curation; **Neal Wade**: Writing – review & editing; **David Greenwood**: Conceptualization, Writing – review & editing, Supervision, Project administration, Funding acquisition

Declaration of competing interest

The authors declare that they have no known competing financial interests or personal relationships that could have appeared to influence the work reported in this paper.

Acknowledgement

This work was supported by the European Union's Horizon 2020 research and innovation programme under grant agreement No 824386.

Appendices

A. Convexification of complex power flow

This section describes the model of the electrical networks used in this paper. The IM and wider distribution network need to be modelled as part of the sizing studies. The complex power flow balance for active power and reactive power injected at bus i is expressed by

$$P_{\text{net},i} = \sum_{k=1}^{N} |V_i||V_k|[G_{ik}cos(\theta_i - \theta_k) + B_{ik}sin(\theta_i - \theta_k)] \quad \text{(A1)}$$

$$Q_{\text{net},i} = \sum_{k=1}^{N} |V_i||V_k|[G_{ik}sin(\theta_i - \theta_k) - B_{ik}sin(\theta_i - \theta_k)] \quad \text{(A2)}$$

where V_i and θ_i denote the voltage and phase angle of bus i, G_{ik} and B_{ik} represent the real and imaginary parts of the element Y_{ik} in the admittance matrix, N is the total number of the buses that connect with bus i. $P_{\text{net},i}$ and $Q_{\text{net},i}$ indicate the net active and reactive power injections at bus i.

According to Ref. [27], by defining variables $u_i = V_i^2/\sqrt{2}$, $R_{ik} = V_iV_kcos(\theta_i - \theta_k)$, $I_{ik} = V_iV_ksin(\theta_i - \theta_k)$, (A1) and (A2) become

$$P_{\text{net},i} = \sqrt{2}G_{ii}u_i + \sum_{\substack{k=1 \\ k\neq i}}^{N} [G_{ik}R_{ik} + B_{ik}I_{ik}] \quad \text{(A3)}$$

$$Q_{\text{net},i} = -\sqrt{2}B_{ii}u_i - \sum_{\substack{k=1 \\ k\neq i}}^{N} [B_{ik}R_{ik} - G_{ik}I_{ik}] \quad \text{(A4)}$$

The ancillary variables R_{ik} and I_{ik} satisfy

$$2u_iu_k = R_{ik}^2 + I_{ik}^2 \quad \text{(A5)}$$

which can be relaxed to

$$2u_iu_k \geq R_{ik}^2 + I_{ik}^2 \quad \text{(A6)}$$

The original nonconvex power flow model is therefore transformed to the convex SOCP model of (A3), (A4) and (A6), which can be efficiently solved to global optimality using commercially available solvers.

B. Modelling of battery degradation

BESS degrade with use [42], and this, crucially, impacts the cost-effectiveness of using the BESS to fulfil use cases [43]; the operating Depth of Discharge (DOD) significantly affects the degradation, hence it is used to explicitly model the battery capacity fade. The model developed in Ref. [28] – which is summarized here – is applied to simulate the battery degradation. The capacity loss ΔE through a single charging/discharging action can be expressed as

$$\Delta E = E_0 \left| D_{\text{ini}}K_{D_{\text{ini}}} - D_{\text{fin}}K_{D_{\text{fin}}} \right| \quad \text{(A7)}$$

where E_0 in (10) is the initial exploitable energy at the beginning of the charging/discharging action, D_{ini} and D_{fin} represent the initial and final DODs. K_D is a coefficient derived from the achievable cycle count (ACC) as a function of operating DOD, provided by the manufacturer. K_D is expressed as

$$K_D = \frac{1}{2D}\left(1 - 0.8^{\frac{1}{N_{ACC(D)}}}\right) \quad \text{(A8)}$$

where $N_{ACC(D)}$ in (A8) is the number of cycles that can be carried out before the battery's exploitable energy capacity reaches 80% of the initial capacity, with a battery operating DOD of D. The battery reaches its end of life when its capacity falls to 80%.

This paper assumes a lithium-ion battery will be deployed in the distribution system. The capacity loss in terms of different initial and final State of Charge (SOC) is obtained as an approximately linear surface. Therefore, a global wear coefficient K_w is developed to approximate K_D and (A7)

$$\Delta E = K_wE\left|D_{\text{ini}} - D_{\text{fin}}\right| \quad \text{(A9)}$$

By calculating the values of ΔE for all possible initial and final SOCs from (A7) and (A9), the root mean squared errors between them are recorded in terms of different values of K_w.

For a lithium battery with lifecycles N_{ACC} decreases from 15,000 to 6000 when the operating DODs increases from 0 to 100%, a value of 1.04×10^{-5} is derived for K_w as the best approximation to (A7) by comparing the root mean squared errors; this means the exploitable capacity reduces approximately 1.04×10^{-5} kWh when the battery charges or discharges by 1 kWh. This method offers accurate estimation of battery degradation while its linearity means it can be included in the optimization problem without modification.

C. Modelling of correlated demand with copula

The demand of customers at different buses in an IM can be strongly correlated because of similar customer behavior and underlying drivers. The correlations can significantly affect the system operation and are explicitly modelled in this section. Based on the historical hourly load data over a year from the case study distribution system, the load of two buses on weekdays in spring from 07:00 to 08:00 are plotted in Fig. A1.

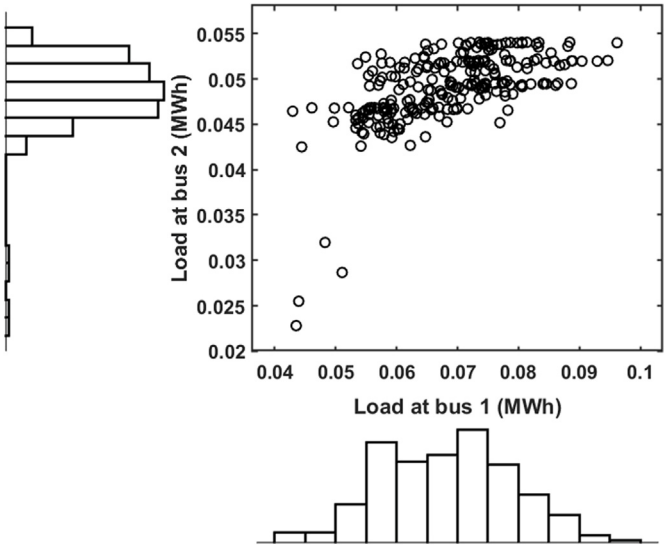

Fig. A1. Hourly weekday loads at bus 1 and 2

Gaussian copula can model the joint distribution with high dimensions, non-linear correlations, and different distributions of uncertain variables [44], hence is appropriate for simulating the correlated loads in a distribution system. This paper applies Gaussian copula to capture the correlations between the load forecast errors at each time step, and subsequently generates correlated copula samples for MCS in solving the CCP.

According to Sklar's theorem, any multi-variate joint distribution with N_ξ variables $F(x_1, x_2, \ldots, x_{N_\xi})$ can be transformed to a copula function $C(x_1, x_2, \ldots, x_{N_\xi})$ in terms of the uniform marginal

distribution of each individual uncertain variable $F_1(x_1)$, $F_2(x_2)$, …, $F_{N_\xi}(x_{N_\xi})$ as shown in

$$F\left(x_1,\ x_2, \ldots,\ x_{N_\xi}\right) = C\left(\left(F_1(x_1), F_2(x_2), \ldots, F_{N_\xi}\left(x_{N_\xi}\right)\right)\right) \quad \text{(A10)}$$

The copula, C, holds the correlations between uncertain variables. By applying Sklar's theorem, the correlations between uncertain variables are captured and transferred to the domain [0, 1]. The inverse transform method can be applied to transfer the copula to the original scale of uncertain variables. Based on these transformations, the correlated samples of uncertain load forecast errors at each time step are generated according to the following procedure:

Step 1) Determine the probability distributions of the load forecast errors at each bus based on historical data. Compute the Spearman's rank correlation coefficients between the errors for each pair of buses.

Step 2) Apply Gaussian copula to fit the historical load forecast errors based on the correlation coefficients, leading to correlated copula on unit scale.

Step 3) Use the inverse transform method and apply the corresponding inverse cumulative distribution function to the correlated copula on unit scale to generate samples of correlated load forecast errors.

References

[1] Ghadi MJ, Rajabi A, Ghavidel S, Azizivahed A, Li L, Zhang J. From active distribution systems to decentralized microgrids: a review on regulations and planning approaches based on operational factors. Appl Energy 2019;253. https://doi.org/10.1016/j.apenergy.2019.113543.

[2] Shang C, Srinivasan D, Reindl T. Generation-scheduling-coupled battery sizing of stand-alone hybrid power systems. Energy 2016;114. https://doi.org/10.1016/j.energy.2016.07.123.

[3] El-Bidairi KS, Nguyen HD, Mahmoud TS, Jayasinghe SDG, Guerrero JM. Optimal sizing of Battery Energy Storage Systems for dynamic frequency control in an islanded microgrid: a case study of Flinders Island, Australia. Energy 2020;195. https://doi.org/10.1016/j.energy.2020.117059.

[4] Huo D, Santos Mv, Greenwood DM, Wade NS, Resch MP. In: Optimal battery sizing for a distribution network in Austria to maximise profits and reliability," in IET Conference Publications; 2020. CP767. https://doi.org/10.1049/oap-cired.2021.0007. 2020.

[5] Sukumar S, Mokhlis H, Mekhilef S, Naidu K, Karimi M. Mix-mode energy management strategy and battery sizing for economic operation of grid-tied microgrid. Energy 2017;118. https://doi.org/10.1016/j.energy.2016.11.018.

[6] H. M. Ridha, C. Gomes, H. Hazim, and M. Ahmadipour, "Sizing and implementing off-grid stand-alone photovoltaic/battery systems based on multi-objective optimization and techno-economic (MADE) analysis," Energy, vol. 207, 2020, doi: 10.1016/j.energy.2020.118163.

[7] Alsaidan I, Khodaei A, Gao W. A comprehensive battery energy storage optimal sizing model for microgrid applications. IEEE Trans Power Syst 2018;33(4). https://doi.org/10.1109/TPWRS.2017.2769639.

[8] Zhang YJA, Zhao C, Tang W, Low SH. Profit-maximizing planning and control of battery energy storage systems for primary frequency control. IEEE Trans Smart Grid 2018;9(2). https://doi.org/10.1109/TSG.2016.2562672.

[9] Elkazaz M, Sumner M, Naghiyev E, Hua Z, Thomas DWP. Techno-Economic Sizing of a community battery to provide community energy billing and additional ancillary services. Sustainable Energy, Grids and Networks 2021;26:100439. https://doi.org/10.1016/j.segan.2021.100439.

[10] Bahramirad S, Reder W, Khodaei A. Reliability-constrained optimal sizing of energy storage system in a microgrid. IEEE Trans Smart Grid 2012;3(4). https://doi.org/10.1109/TSG.2012.2217991.

[11] Mitra J, Vallem MR. Determination of storage required to meet reliability guarantees on island-capable microgrids with intermittent sources. IEEE Trans Power Syst 2012;27(4). https://doi.org/10.1109/TPWRS.2012.2203831.

[12] Luo Y, Shi L, Tu G. Optimal sizing and control strategy of isolated grid with wind power and energy storage system. Energy Convers Manag 2014;80. https://doi.org/10.1016/j.enconman.2014.01.061.

[13] Astaneh M, Roshandel R, Dufo-López R, Bernal-Agustín JL. A novel framework for optimization of size and control strategy of lithium-ion battery based off-grid renewable energy systems. Energy Convers Manag 2018;175. https://doi.org/10.1016/j.enconman.2018.08.107.

[14] Arabali A, Ghofrani M, Etezadi-Amoli M, Fadali MS. Stochastic performance assessment and sizing for a hybrid power system of Solar/Wind/Energy Storage. IEEE Trans Sustain Energy 2014;5(2). https://doi.org/10.1109/TSTE.2013.2288083.

[15] Awad ASA, EL-Fouly THM, Salama MMA. Optimal ESS allocation for benefit maximization in distribution networks. IEEE Trans Smart Grid 2017;8(4). https://doi.org/10.1109/TSG.2015.2499264.

[16] Zografou-Barredo NM, Patsios C, Sarantakos I, Davison P, Walker SL, Taylor PC. MicroGrid resilience-oriented scheduling: a robust misocp model. IEEE Trans Smart Grid 2021;12(3). https://doi.org/10.1109/TSG.2020.3039713.

[17] Greenwood DM, Wade NS, Taylor PC, Papadopoulos P, Heyward N. A probabilistic method combining electrical energy storage and real-time thermal ratings to defer network reinforcement. IEEE Trans Sustain Energy 2017;8(1). https://doi.org/10.1109/TSTE.2016.2600320.

[18] Yu H, Chung CY, Wong KP, Zhang JH. A chance constrained transmission network expansion planning method with consideration of load and wind farm uncertainties. IEEE Trans Power Syst 2009;24(3). https://doi.org/10.1109/TPWRS.2009.2021202.

[19] Zhang Y, Lundblad A, Campana PE, Benavente F, Yan J. Battery sizing and rule-based operation of grid-connected photovoltaic-battery system: a case study in Sweden. Energy Convers Manag 2017;133. https://doi.org/10.1016/j.enconman.2016.11.060.

[20] Khorramdel H, Aghaei J, Khorramdel B, Siano P. Optimal battery sizing in microgrids using probabilistic unit commitment. IEEE Trans Ind Inf 2016;12(2). https://doi.org/10.1109/TII.2015.2509424.

[21] Ehsan A, Yang Q. Coordinated investment planning of distributed multi-type stochastic generation and battery storage in active distribution networks. IEEE Trans Sustain Energy 2019;10(4). https://doi.org/10.1109/TSTE.2018.2873370.

[22] Atia R, Yamada N. Sizing and analysis of renewable energy and battery systems in residential microgrids. IEEE Trans Smart Grid 2016;7(3). https://doi.org/10.1109/TSG.2016.2519541.

[23] Bordin C, Tomasgard A. SMACS MODEL, a stochastic multihorizon approach for charging sites management, operations, design, and expansion under limited capacity conditions. J Energy Storage Dec. 2019;26:100824. https://doi.org/10.1016/J.EST.2019.100824.

[24] Xie C, Wang D, Lai CS, Wu R, Wu X, Lai LL. Optimal sizing of battery energy storage system in smart microgrid considering virtual energy storage system and high photovoltaic penetration. J Clean Prod 2021;281:125308. https://doi.org/10.1016/j.jclepro.2020.125308.

[25] Gong K, Wang X, Jiang C, Shahidehpour M, Liu X, Zhu Z. Security-constrained optimal sizing and siting of BESS in hybrid AC/DC microgrid considering post-contingency corrective rescheduling. IEEE Trans Sustain Energy 2021;12(4). https://doi.org/10.1109/TSTE.2021.3080707.

[26] El-Bidairi KS, Duc Nguyen H, Jayasinghe SDG, Mahmoud TS, Penesis I. A hybrid energy management and battery size optimization for standalone microgrids: a case study for Flinders Island, Australia. Energy Convers Manag 2018;175. https://doi.org/10.1016/j.enconman.2018.08.076.

[27] Jabr RA. Radial distribution load flow using conic programming. IEEE Trans Power Syst 2006;21(3). https://doi.org/10.1109/TPWRS.2006.879234.

[28] Farzin H, Fotuhi-Firuzabad M, Moeini-Aghtaie M. A practical scheme to involve degradation cost of lithium-ion batteries in vehicle-to-grid applications. IEEE Trans Sustain Energy 2016;7(4). https://doi.org/10.1109/TSTE.2016.2558500.

[29] Hatziargyriou N, et al. Definition and classification of power system stability - revisited & extended. IEEE Trans Power Syst 2021;36(4). https://doi.org/10.1109/TPWRS.2020.3041774.

[30] Escalera A, Hayes B, Prodanović M. A survey of reliability assessment techniques for modern distribution networks. Renew Sustain Energy Rev 2018;91. https://doi.org/10.1016/j.rser.2018.02.031.

[31] Santos M, Huo D, Wade N, Greenwood D, Sarantakos I. Reliability assessment of island multi-energy microgrids. Energy Conversion and Economics 2021;2(3). https://doi.org/10.1049/enc2.12040.

[32] Billinton R, Li W. Reliability assessment of electric power systems using Monte Carlo methods. 1994. https://doi.org/10.1007/978-1-4899-1346-3.

[33] D. Huo, C. Gu, D. Greenwood, Z. Wang, P. Zhao, and J. Li, "Chance-constrained optimization for integrated local energy systems operation considering correlated wind generation," Int J Electr Power Energy Syst, vol. 132, 2021, doi: 10.1016/j.ijepes.2021.107153.

[34] Baker K, Hug G, Li X. Energy storage sizing taking into account forecast uncertainties and receding Horizon operation. IEEE Trans Sustain Energy 2017;8(1). https://doi.org/10.1109/TSTE.2016.2599074.

[35] Lu X, Chan KW, Xia S, Zhang X, Wang G, Li F. A model to mitigate forecast uncertainties in distribution systems using the temporal flexibility of EVAs. IEEE Trans Power Syst 2020;35(3). https://doi.org/10.1109/TPWRS.2019.2951108.

[36] Integrated Modular energy systems and local Flexibility trading for Neural energy islands (MERLON), available at *https://www.merlon-project.eu/*".

[37] Gurobi LLC. Optimization, "Gurobi optimizer reference manual. 2020. https://www.gurobi.com/documentation/9.0/refman/index.html. *aufgerufen am 27.10.2020*.

[38] Technische und Organisatorische Regeln für Betreiber und Benutzer von Netzen (TOR), E-CONTROL, available at *https://www.e-control.at/recht/marktregeln/tor*".

[39] SEDC Report 2017: Explicit demand response in Europe – Mapping the markets, available at *https://www.etip-snet.eu/sedc-report-2017-mapping-demand-response-europe-today/*".

[40] Fleer J, Stenzel P. Impact analysis of different operation strategies for battery energy storage systems providing primary control reserve. J Energy Storage

2016;8. https://doi.org/10.1016/j.est.2016.02.003.
[41] Schröder T, Kuckshinrichs W. Value of lost load: an efficient economic indicator for power supply security? A literature review. Front Energy Res 2015;3. https://doi.org/10.3389/fenrg.2015.00055. DEC.
[42] Aaslid P, Belsnes MM, Fosso OB. In: Optimal microgrid operation considering battery degradation using stochastic dual dynamic programming," in 2019 International Conference on Smart Energy Systems and Technologies. SEST); 2019. p. 1–6. https://doi.org/10.1109/SEST.2019.8849150.
[43] Bordin C, Anuta HO, Crossland A, Gutierrez IL, Dent CJ, Vigo D. A linear programming approach for battery degradation analysis and optimization in offgrid power systems with solar energy integration. Renew Energy Feb. 2017;101:417–30. https://doi.org/10.1016/J.RENENE.2016.08.066.
[44] Xie ZQ, Ji TY, Li MS, Wu QH. Quasi-Monte Carlo based probabilistic optimal power flow considering the correlation of wind speeds using copula function. IEEE Trans Power Syst 2018;33(2). https://doi.org/10.1109/TPWRS.2017.2737580.